

Synthesis and X-ray Crystallography of Rh(I) Carbonyl Complexes of Amethyrin

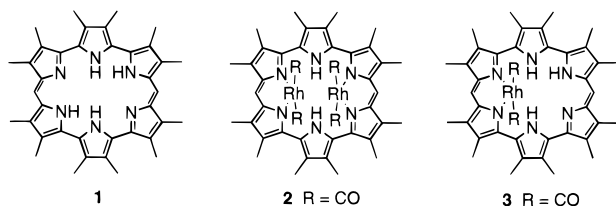
Jonathan L. Sessler,* Andreas Gebauer, Anka Guba, Markus Scherer, and Vincent Lynch

Department of Chemistry and Biochemistry,
University of Texas at Austin, Austin, Texas 78712

Received August 13, 1997

Introduction

Amethyrin (e.g., **1**) is a stable, six pyrrole containing, 24 π -electron conjugated expanded porphyrin.¹ Due to its six



inward-pointing chelating nitrogen atoms, a variety of different metal coordination modes can, at least in theory, be conceived for this potentially binucleating ligand. These range from η^2 to η^6 as illustrated by structures I–V in Figure 1.

To date, two η^2 complexes of amethyrin with cobalt(II)¹ and zinc(II)¹ and one η^3 complex with copper(II)² have been synthesized. These complexes served to show that the amethyrin macrocycle is able not only to rearrange its π -conjugation pathway through a tautomeric shift of protons¹ but also to distort its scaffold, by a transverse in-plane “slipping” of two pyrroles, so as to accommodate a given metal coordination environment.² While rearrangements of the π -conjugation pathway have been observed previously in the case of certain heterosapphyrins,³ the within-plane shifting distortions observed with amethyrin appear to be unprecedented in the chemistry of conjugated expanded porphyrins. In light of this, we are continuing to explore further the basic metal coordination behavior of amethyrin. Here, we report the synthesis of two Rh(I) complexes, mono and bis, of this seemingly unique hexaaza ligand system. The impetus for this work came from a desire to assess the extent to which complexation of one or more rhodium(I) cations could be used to influence the overall ligand geometry.

Results and Discussion

The reaction of amethyrin **1** in dry dichloromethane containing triethylamine as the auxiliary base with an excess of μ -dichloro-bis(rhodiumdicarbonyl) led to the formation of complexes **2** and **3**. These species were isolated via column chromatography on neutral alumina using dichloromethane and dichloromethane/hexanes 1/3 (v/v), respectively, as the eluents.

The first complex we were able to isolate and characterize by X-ray crystallography was the bis-Rh(I)–amethyrin complex **2**. Surprisingly, and in contrast to what is seen for dirhodium(I) complexes of octaethylporphyrin,⁴ sapphyrin,⁵ and various heterosapphyrins,³ in this structure both of the rhodium atoms lie on the same, convex side of the bowl-shaped macrocycle (see Figure 2).⁶ Nonetheless (i.e., despite this cis-like configuration), the two rhodium centers remain separated from one another by a considerable distance, namely ~ 4.1 Å. It is thus clear, at least in the solid state, that there is little or no interaction between the metal centers.

While initially unexpected, the bowl-shaped structure of the macrocycle can be rationalized in terms of repulsive interactions involving the “opposite” carbonyl groups (2A–2D and 2B–2C). The contact distances for these two carbonyl units, of 3.071(3) and 3.025(3) Å for 2A–2D and 2B–2C, respectively, lie in the range expected range for the sum of van der Waals radii (i.e., 2.9–3.4 Å).⁷ As far as the metal centers are concerned, complex **2** displays a slightly distorted square planar coordination for the rhodium atoms. The Rh1 atom is located 0.119 Å out of the N1–N6–C2A–C2B mean least-squares plane, whereas Rh2 is found to lie 0.143 Å out of the N3–N4–C2C–C2D mean least-squares plane.

The angle between the planes defined by the two dipyrromethene-like subunits of the amethyrin macrocycle is 46.4°. Both Rh atoms are located about 1.1 Å above these two planes in a location that can be considered trans to the center pyrroles of the terpyrrole subunits. This binding, which is accompanied by a concomitant rotation of these center pyrrolic moieties in opposite directions, results in an overall bending of the amethyrin framework (Figure 2). These center pyrroles form an angle of $\sim 36.7^\circ$ with their neighboring pyrroles. The distance between the rhodium atoms and the nitrogens in complex **2** is about 2.06 Å.

Solid-state structural information could also be obtained for the mono-Rh(I)–amethyrin complex **3**. X-ray crystallography revealed a structure similar to that observed for the bis-Rh(I)–amethyrin complex **2**. Specifically, complex **3** is found to adopt a bowl-shaped conformation in the solid state (see Figure 3). Interestingly, it does so in spite of the fact that only one rhodium(I) center is bound. In this instance, the center pyrroles of the terpyrrole subunits form an angle of $\sim 35^\circ$ with their neighboring pyrroles. However, because the crystals were found to be disordered, with an 85% relative occupancy found for one of the two possible metal coordination sites, these angles should be considered accurate only in an average sense. In any event, the angle between the planes defined by the dipyrromethane subunits is 32.2°, a value that is smaller than that seen in **2**. The reduction in this angle can be rationalized in terms of the reduced steric bulk that arises as the result of having

(1) Sessler, J. L.; Weghorn, S. J.; Hiseada, Y.; Lynch, V. *Chem.—Eur. J.* **1995**, *1*, 56.

(2) Weghorn, S. J.; Sessler, J. L.; Lynch, V.; Baumann, T. F.; Sibert, J. W. *Inorg. Chem.* **1996**, *35*, 1089.

(3) Sessler, J. L.; Burrell, A. K.; Lisowski, J.; Gebauer, A.; Cyr, M. J.; Lynch, V. *Bull. Soc. Chim. Fr.* **1996**, *133*, 725.

(4) (a) Takenaka, A.; Sasada, Y. *J. Chem. Soc., Chem. Commun.* **1973**, 792. (b) Takenaka, A.; Sasada, Y.; Ogoshi, H.; Omura, T.; Yoshida, Z.-I. *Acta Crystallogr.* **1973**, *B31*, 1. (c) Brothers, P. J.; Collman, J. P. *Acc. Chem. Res.* **1986**, *19*, 209.

(5) Burrell, A. K.; Sessler, J. L.; Cyr, M. J.; McGhee, E.; Ibers, J. A. *Angew. Chem., Int. Ed. Engl.* **1991**, *30*, 91.

(6) A bowl-like structure with cis coordination of the metal center has been observed previously in the case of another nonaromatic expanded porphyrin–rhodium(I) complex. This system, in contradistinction from the present work, involved a ligand that was not fully conjugated; see the following: Carré, F. H.; Corriu, R. J. P.; Bolin, G.; Moreau, J. J. E.; Vernhet, C. *Organometallics* **1993**, *12*, 2478.

(7) Bondi, A. *J. Phys. Chem.* **1964**, *68*, 441.

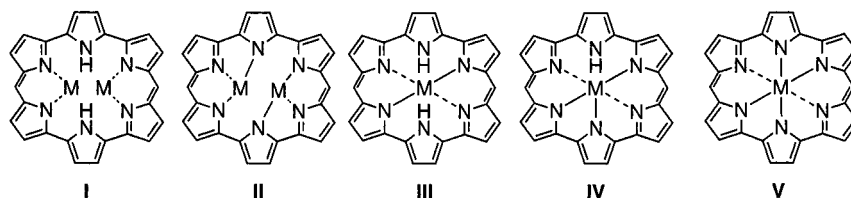


Figure 1. Possible binding modes for mono- and binuclear amethyrin metal complexes.

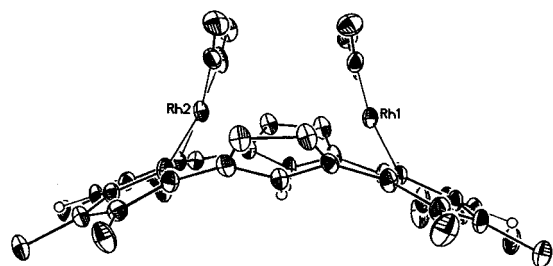
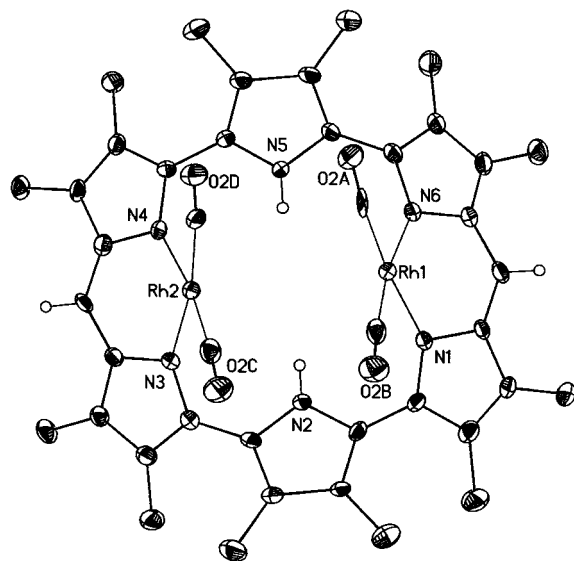


Figure 2. Front and side views of $C_{38}H_{40}N_6[Rh(CO)_2]_2$ (**2**) showing the heteroatom labeling scheme. Thermal ellipsoids are scaled to the 30% probability level. H atoms are scaled to an arbitrary size. In the side view, the β -methyl substitutions on the central pyrrolic moieties have been omitted for clarity.

only one metal center bound. This reduction in steric bulk is also reflected in the slightly longer distances between the rhodium atom and the nitrogens in complex **3**; these latter distances average 2.1 Å.

While the above differences between **2** and **3** are noteworthy, the most striking conclusion that comes out of such a structural comparison is the fact that steric effects associated with the carbonyl groups are only in part responsible for the bowl shape of the amethyrin macrocycle. Another important factor is the maintenance of the preferred ligand environment about the rhodium(I) metal center. Restated, complex **3** adopts a bowl shape because the rhodium(I) atom and the two ancillary carbonyl ligands cannot fit into the macrocyclic plane while still retaining a net square planar geometry around the Rh(I) center.⁸ Thus, in this instance, the steric requirements of Rh(I) coordination take preference over those associated with macrocycle distortion. Amethyrin differs in this regard from other expanded porphyrin systems such as sapphyrin.⁹

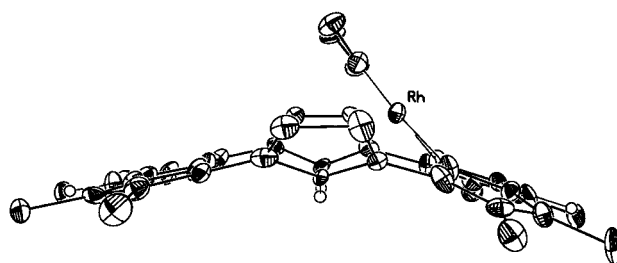
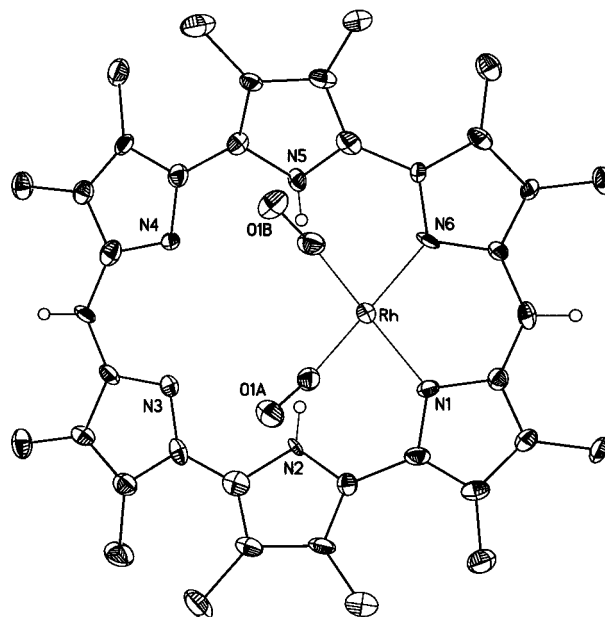


Figure 3. Front and side views of $C_{38}H_{40}N_6Rh(CO)_2$ (**3**) showing the heteroatom labeling scheme. Thermal ellipsoids are scaled to the 30% probability level. H atoms are scaled to an arbitrary size. In the side view, the β -methyl substitutions on the central pyrrolic moieties have been omitted for clarity.

The UV/vis spectra of **2** and **3** show features expected for an expanded porphyrin–metal complex. For instance, Soret-type bands at 424 (for **2**) and 426 nm (for **3**) are observed that are weaker than those for the corresponding free base system, **1**. Likewise Q-type bands are seen at 516 (for **2**) and 536 nm (for **3**) that are stronger than those of **1**. While complex **3** also displays an additional shoulder at 517 nm, its absorptions are weaker overall than those of **2**.

Both compound **2** and compound **3**, like the analogous sitting-a top porphyrin and sapphyrin metal carbonyl complexes,^{4,5} are diamagnetic. Well-resolved ¹H NMR and ¹³C NMR spectra could thus be recorded. As might be expected, these spectra not only provided further proof of structure but also served to provide the solution state conformational properties of these complexes. In the specific case of **2**, such studies

(8) Holleman, A. F., Wiberg, N., Eds. *Lehrbuch der Anorganischen Chemie*; Walter de Gruyter: Berlin, 1985; p 1198.

(9) Interestingly, in CD_2Cl_2 only one broad meso proton signal is observed in the ¹H NMR spectrum. This is consistent with the rate of cis/trans isomer interconversion being faster in this solvent.

revealed a system possessing more than one conformational state in solution. For example, two singlets were observed for the meso protons in the ^1H NMR spectrum of **2**. However, were the molecule to possess the symmetry seen in the X-ray structure, one would expect to observe only one signal. The ^{13}C NMR spectrum of **2** also contains 33 well-resolved signals instead of the 10 expected for a symmetric structure akin to what is seen in the solid state.

To obtain a better understanding of the processes taking place in solution variable temperature ^1H NMR, studies of the bis-rhodium complex **2** in toluene- d_8 were undertaken. Surprisingly, little difference was seen in spectra recorded at room temperature and at 60 °C.⁹ In fact, the two signals observed for the meso-protons show no change at all. Such findings are consistent with the existence of two stable species in solution which do not interconvert into one another (on the NMR time scale) either at room temperature or at 60 °C. This, in turn, leads us to propose that a second postulated species, the corresponding *trans*-bis rhodium(I)dicarbonyl complex (wherein the two metal centers are found on opposite sides of the mean amethyryn plane) exists in solution. While such *trans* structures are well documented in the case of porphyrins and sapphyrins,^{4,5} in the present instance only the *cis* complex has been isolated in the solid state.¹⁰

In the case of **3** the ^1H NMR and ^{13}C NMR spectra are consistent with the corresponding solid-state X-ray crystal structure. This is not surprising since in this instance only one half of the amethyryn macrocycle is locked in a bowl-like conformation while the other half can rotate freely even, presumably, at low temperature. Thus, even if chair-like structures are formed in a transient way, the time-averaged NMR spectra would reflect, at least in terms of gross symmetry, the structure seen in the solid state.

The present results serve to confirm further the versatility of amethyryn as a metal-coordinating ligand. Specifically, we have shown in this Note that amethyryn can stabilize both mono- and bis-metallic out-of-plane complexes with rhodium(I). Both metal complexes display a bowl-like conformation as far as the ligand is concerned and are normal with regard to the nature of the η^2 coordination involving each rhodium center. Surprisingly, however, in the case of the bis-metallic system **2**, a rather unusual *cis*-like arrangement of the two metal centers is observed. Such a configuration is not observed in either porphyrin or sapphyrin, the best-studied expanded porphyrin analogue. The present results thus serve to demonstrate in quite graphic fashion how small changes in polypyrrole structure can end up having a profound influence on the specifics of the metal chelation behavior. This is a theme we are continuing to develop in our laboratory.

Experimental Section

General. Melting points were determined on a Mel-Temp melting point apparatus and are uncorrected. Proton and ^{13}C NMR spectra were measured at 25 °C on a GE QE-300 spectrometer at 300 and 75.5

MHz or at 25 °C on a Bruker AMX-500 spectrometer at 500 and 125 MHz, respectively. UV/vis spectra were recorded on a Beckman DU-650 spectrophotometer. Low-resolution FAB mass spectra were obtained on a Finnigan MAT TSQ 70 mass spectrometer. High-resolution FAB mass spectra were obtained on a VGZ AB-E mass spectrometer. FAB spectra were obtained using a nitrobenzyl alcohol (NBA) matrix. Dichloromethane and methanol were dried over calcium hydride. All other reagents were used as received.

Bis-rhodium(I)-3,4,8,9,12,13,16,17,21,22,25,26-dodecamethylamethyryn-tetracarbonyl (2) and Rhodium(I)-3,4,8,9,12,13,16,17,21,22,25,26-dodecamethylamethyryn-dicarbonyl (3). In a 100-mL round-bottomed flask, equipped with an argon inlet, 3,4,8,9,12,13,16,17,21,22,25,26-dodecamethylamethyryn¹ (**1**) (free base form; 74 mg, 0.13 mmol) was dissolved in dry dichloromethane (30 mL). Triethylamine (2 mL) was added, followed by $[\text{RhCl}(\text{CO})_2]_2$ (247 mg, 0.64 mmol) dissolved in dry methanol (20 mL). The yellow-brown solution immediately turned deep red. The resulting mixture was stirred overnight at room temperature. The residual solvent and excess triethylamine were then removed *in vacuo*. The residue was taken up in a small amount of dichloromethane and purified chromatographically on neutral alumina (column length: 2 cm \times 15 cm) using dichloromethane as the eluant. The first pink-red fraction (running with the solvent front) was collected and taken to dryness *in vacuo*. As judged by thin-layer chromatography (TLC), this product was not homogeneous. Therefore, this material was again purified chromatographically, this time using a neutral alumina column (2 cm \times 10 cm) and dichloromethane/*n*-hexane 1/3 (v/v) as the eluent. The first orange-red fraction (bis-rhodium(I) complex, **2**) and the second pink-red fraction (mono-rhodium(I) complex, **3**) were collected separately, and in each case, the solvent evaporated off under reduced pressure. The respective residues were redissolved in dichloromethane and layered with *n*-hexane to give independently the bis-rhodium(I) adduct, **2**, as metallic green crystals (47 mg, 41% yield) and the mono-rhodium(I) adduct, **3**, as metallic green crystals (8 mg, 8.5% yield).

For 2. Mp: dec > 220 °C. ^1H NMR (500 MHz, toluene- d_8): δ 1.52 (s, 6H), 1.57 (s, 6H), 1.60 (s, 6H), 1.61 (s, 6H), 1.63 (s, 6H), 1.69 (s, 6H), 1.69 (s, 6H), 1.70 (s, 6H), 1.77 (s, 6H), 1.79 (s, 6H), 1.82 (s, 6H), 1.87 (s, 6H), 5.80 (s, 2H), 6.11 (s, 2H), 12.51 (bs, 2H). ^{13}C NMR (75.5 MHz, CDCl_3): δ 9.1, 9.2, 9.6, 9.7, 9.9, 10.0, 10.4, 11.3, 11.4, 115.5, 120.4, 120.5, 125.7, 126.0, 126.5, 126.7, 126.8, 127.04, 128.15, 128.8, 129.0, 130.5, 136.2, 137.63, 140.76, 140.9, 142.6, 143.5, 148.8, 153.2, 159.5, 161.8, 184.4, 184.9, 185.5, 186.0. IR (KBr): 2015, 2067 (CO), 2845, 2923, 2953, 3317, 3397 cm^{-1} . UV/vis (CH_2Cl_2): λ_{max} [nm] 424 ($\epsilon = 32\,974$), 516 ($\epsilon = 53\,540$). HRMS (FAB +) *m/e* calcd for $\text{C}_{42}\text{H}_{40}\text{N}_6\text{O}_4\text{Rh}_2$: 898.1221. Found: 898.1216.

For 3. Mp: dec > 220 °C. ^1H NMR (500 MHz, CDCl_3): δ 1.23 (s, 3H), 1.55 (s, 6H), 1.58 (m, 9H), 1.68 (s, 6H), 1.73 (s, 6H), 1.79 (s, 6H), 1.86 (s, 6H), 5.28 (bs, 2H), 5.49 (s, 1H), 5.81 (s, 1H), 13.66 (bs, 2H). ^{13}C NMR (75.5 MHz, CDCl_3): δ 9.4, 9.8, 10.2, 10.2, 10.8, 29.7, 124.3, 125.8, 125.9, 126.1, 126.5, 126.7, 127.5, 136.2, 136.9, 139.7, 140.7, 148.6, 158.0, 184.7, 185.2. IR (KBr): 2015, 2067 (CO), 2845, 2923, 2953, 3317, 3397 cm^{-1} . UV/vis (CH_2Cl_2): λ_{max} [nm] 426 ($\epsilon = 17\,691$), 517 (sh, $\epsilon = 25\,300$), 536 ($\epsilon = 26\,683$). HRMS (FAB +) *m/e* calcd for $\text{C}_{40}\text{H}_{41}\text{N}_6\text{O}_2\text{Rh}$: 740.2346. Found: 740.2336.

X-ray Structure Determination. Crystals of **2** grew as very dark needles by layering a small amount of hexanes over a solution in CH_2Cl_2 (crystal used, 0.23 \times 0.29 \times 0.60 mm). Crystals of **3** grew as dark green blocks by slow evaporation from CH_2Cl_2 (crystal used, 0.15 \times 0.16 \times 0.17 mm). The data were collected at -75 and -80 °C for **2** and **3**, respectively, on a Siemens P3 diffractometer, equipped with a Nicolet LT-2 low-temperature device and using a graphite monochromator with Mo K α radiation ($\lambda = 0.710\,73\text{ \AA}$). Four reflections for **2** (3, -1, 3; 2, 5, 4; -1, -4, 1; -4, -2, -6) and for **3** (-4, -1, 1; 2, -3, 1; 4, 1, -1; -4, 1, 1) were remeasured every 96 reflections to monitor instrument and crystal stability. A smoothed curve of the intensities of these check reflections was used to scale the data. The scaling factor ranged from 0.9694 to 1.000 for **2** and from 0.9147 to 0.9455 for **3**. The data of **2** were corrected for Lp effects and absorption. The absorption correction was based on crystal shape measurements. The data of **3** were corrected for Lp effects but not for absorption. Data reduction, decay and absorption correction, structure

(10) Two possible explanations for this observation come immediately to mind. First, the *cis* complex could be less soluble in the solvents chosen for crystallization and therefore crystallized as the only species. Alternatively, it could be that both the *cis* and the *trans* complexes crystallized but that a crystal of the *cis* complex was arbitrarily chosen for the X-ray crystallographic analysis. In an attempt to address this issue the UV/vis spectra of both the crystals (redissolved in CH_2Cl_2) and the filtrate were recorded and found to be the same. Because of this congruence, it is difficult at present to ascertain whether the filtrate was in fact enriched in *trans* isomer. Analogous experiments involving ^1H NMR analyses could not be carried out effectively due to lack of sample.

solution and refinement were performed using the SHELXTL/PC software package.¹¹ The structure was solved by direct methods and refined by full-matrix least squares on F^2 with anisotropic displacement parameters for the non-H atoms. The hydrogen atoms were calculated in idealized positions (C–H, 0.96 Å; N–H, 0.90 Å) with isotropic displacement parameters set to $1.2U_{\text{eq}}$ of the attached atom ($1.5U_{\text{eq}}$ for methyl hydrogen atoms). The function, $\sum w(|F_o|^2 - |F_c|^2)^2$, was minimized, where $w = 1/[(\sigma(F_o))^2 + (0.02P)^2]$ and $P = (|F_o|^2 + 2|F_c|^2)/3$. The data of **2** were not corrected for secondary extinction effects, as this effect was determined to be negligible. The data of **3** were corrected for secondary extinction effects. The correction takes the form: $F_{\text{corr}} = kF_o/[1 + (5(2) \times 10^{-6})F_c^2 \lambda^3/\sin(2\theta)]^{0.25}$, where k is the overall scale factor. Neutral atom scattering factors and values used to calculate the linear absorption coefficient are from the *International Tables for X-ray Crystallography* (1992).¹² Other computer programs

(11) Sheldrick, G. M. *SHELXTL/PC* (Version 5.03); Siemens Analytical X-ray Instruments, Inc.: Madison, WI, 1994.

used in this work are listed elsewhere.¹³ All figures were generated using SHELXTL/PC.¹¹

Acknowledgment. This work was supported by NSF Grant CHE 9725399 to J.L.S. and an Alexander von Humboldt fellowship to M.S.

Supporting Information Available: X-ray experimental and tables of crystallographic data, collection procedures, and parameters, complete atomic coordinates, bond distances and angles, torsion angles, and least-squares planes (43 pages). Ordering information is given on any current masthead page.

IC971018M

(12) *International Tables for X-ray Crystallography*; Wilson, A. J. C., Ed.; Kluwer Academic Publishers: Boston, 1992; Vol. C, Tables 4.2.6.8 and 6.1.1.4.

(13) Gadol, S. M.; Davis, R. E. *Organometallics* **1982**, *1*, 1607–1613.